Selective sorption of divalent cations using a high capacity sorbent

Alan J. Du [a], Darren D. Sun [a,*], James O. Leckie [b]

[a] School of Civil and Environmental Engineering, Nanyang Technological University, 50 Nanyang Avenue, Singapore 639798, Republic of Singapore
[b] Department of Civil and Environmental Engineering, Stanford University, Stanford, CA 94305, USA

ARTICLE INFO

ABSTRACT

This manuscript describes the application of a novel sorbent, sodium titanate nanotube (STN) on partitioning of various divalent cations. Seven divalent cations, from alkaline earth, transition and post-transition groups, were used to determine the capacity and selectivity of STN. At pH 3 ± 0.02 and 0.1 M ionic strength, STN displayed high capacity for Pb and Cd (1.27 and 0.39 mmol/g, correspondingly). The affinity of divalent cations was in the order $Pb \gg Cd > Cu > Zn > Ca > Sr > Ni$. For six of the tested cations, their sorption capacity can be linearly correlated to its hydrolysis constant and electronegativity. STN has unusually low affinity for Ni and correlations of sorption capacity of Ni falls outside the 95% confidence intervals. Furthermore, it exhibited sorption behavior similar to alkaline earth cations, significant uptakes occurred only when pH > point of zero charge. In competitive sorption tests, STN preferentially sorb Cd over other metals (Zn, Ni, Ca and Sr) which coexist in industrial wastewater. As such STN is a potential novel sorbent useful for partitioning Cd from other metals in industrial wastewater.

1. Introduction

Cadmium is widely used in industries such as plastics manufacturing, batteries, pigments, metal alloys and pesticides [1]. World's cadmium production increased from 17,500 tonnes in 2002 to 21,100 tonnes in 2006 [2]. It is estimated that 75% of total cadmium consumption was for the production of rechargeable nickel–cadmium (NiCd) batteries [3]. Despite the introduction of lithium-ion and nickel-metal hydride substitutes to consumer electronic products, NiCd batteries remain in demand for industrial applications [4]. Indeed, cadmium becomes a common occurrence in wastewater of the industry and in view of this, USEPA [5] has enforced strict regulations on cadmium levels in industrial discharges.

In Japan, the infamous itai-itai disease is the result of using cadmium-tainted river water for irrigation purposes. Symptoms of cadmium poisoning are characterized by kidney damage (renal tubular dysfunction) and softening of bones (osteomalacia) in the victims [6]. Moreover, cadmium is a human carcinogen causing cancer of the lung, kidney and prostate. The heavy metal has a long biological half-life in humans and is able to accumulate in the human long after the exposure period [7]. Due to its high toxicity to humans, cadmium pollution is of significant concern.

Commercial ion-exchange resins are often used to sorb heavy metals. Matrix are usually styrene divinylbenzene copolymer grafted with sulfonate [8], iminodiacetate or thiol [9] groups. They have high capacity for heavy metals but low selectivity. Cadmium, however, often coexists with many other cations in wastewater and the resins' non-selective sorption of every heavy metal becomes operationally inefficient. It results in depletion of sites for partitioning of more toxic ions and impedes the process of recovering the more precious metal. In order to recover valuable metals of high purity from spent sorbent, the sorbent itself needs to have high selectivity in addition to high capacity.

Nanotubular titanate was discovered by Kasuga et al. [10] in 1998. Since its finding, titanate nanotube has been recognized as a potentially effective sorbent. It was applied to sorb various aqueous ions and studies have shown that titanate nanotube is able to partition heavy metals [11,12], radionuclides [13], alkali metals [14] and other pollutants [15,16]. However there is a lack of information concerning the cation selectivity of this novel sorbent. This manuscript reports sorption capacities of STN for seven divalent cations (Ca, Ni, Cu, Zn, Sr, Cd and Pb). Correlations of sorption capacities were made with various intrinsic parameters of the cations. Competitive sorptions were conducted to elucidate the sorption selectivity of STN on cadmium. This manuscript aims to use empirical approaches (Langmuir isotherm, Kurbatov plot and the theory of hard soft acids and bases (HSAB)) to describe interactions between STN-divalent cations and correlate observations with intrinsic parameters of cations.

2. Materials and methods

2.1. Chemicals

All chemicals are reagent grade unless otherwise stated. Sodium hydroxide (NaOH) pellets were supplied by VWR BDH. Titanium dioxide (Merck) was used as precursor for the synthesis of sodium titanate nanotubes (STNs). Synthesis procedure was modified version of Kasuga et al. [10], typically 4 g of TiO_2 powder was added to 50 mL NaOH solution (10 M). The mixture was stirred for 1 day and loaded into an acid digestion bomb (125 mL, Parr Instruments) for 2 days at 150 °C. As-synthesized STN were retrieved from the Teflon cup and washed with de-ionized water in a 1 L HDPE bottle. After 1 day, the STN were separated (centrifuged at 10,000 rpm for 30 min) and washed with de-ionized water. The washing process was repeated until solution has neutral pH and a conductivity of 10^{-6} S/cm. The STN were freeze dried and added into de-ionized water to form slurry of known concentration. The slurry was subjected to conditioning in an end-over-end mixer for 2 weeks. To ensure a homogenous STN stock the slurry was transferred to a settling column to separate larger aggregates. After 30 min the supernatant in the column was retrieved and the concentration of STN in supernatant was calculated by determining the dry weight of the settled particles. The final STN had a point of zero charge (PZC) of 6.5 and BET surface area of 206 ± 2.4 m^2/g.

2.2. Equipments

All cations were measured by inductively coupled plasma optical emission spectroscopy (ICP-OES, PerkinElmer Optima 2000). Using standard solutions, a 5-point calibration is performed prior to every measurement.

2.3. Experiments

Isotherm and sorption edge experiments were conducted using 20 mL samples with appropriate concentrations of STN and ionic strength. The solutions were spiked with divalent cations and subjected to end-over-end mixing for 24 h in the dark. In kinetic studies (not shown), it is found that equilibrium was achieved within 10 min of sorption. Nevertheless, pseudo-equilibrium duration of 24 h was used throughout all batch tests for consistency purpose. After equilibration, pH was measured and the samples were then subjected to centrifugation at 10,000 rpm, 30 min. Controls were used for all tests.

3. Results and discussion

3.1. Sorption isotherms

STN sorption capacities for seven divalent cations, Ca, Ni, Cu, Zn, Sr, Cd and Pb, were measured from the Langmuir sorption isotherms. In this work the experiments were conducted at pH 3 to ensure cation removal is through sorption instead of surface precipitation. The low pH also ensures the pH values before and after sorption do not deviate significantly ($\pm$ 0.02 pH units). Fig. 1 shows the experimental data and respective sorption isotherms. Every set of data points was well fitted by Langmuir isotherm:

$$\Gamma = \frac{\Gamma_{max} K_L C_e}{1 + K_L C_e}$$

where Γ is the amount of cation sorbed at equilibrium (mol/g), Γ_{max} is the sorption capacity of STN, K_L is Langmuir sorption constant (L/mol) and C_e is the concentration of solution cation at equilibrium (mol/L). Langmuir isotherm describes sorbate forming monolayer on the sorbent surface. Hydroxyl groups at STN surface
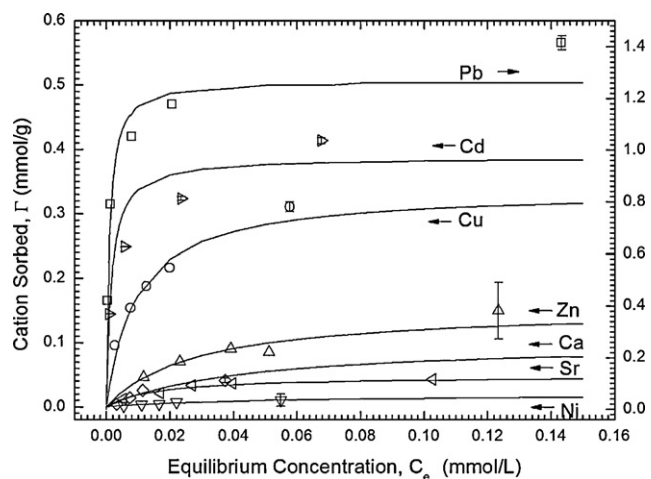

Fig. 1. Sorption isotherms of divalent cations on STN. Lines are Langmuir isotherms. Error bars represent standard deviation of triplicates. STN = 0.05 g/L, I = 0.1 M, pH 3 ± 0.02.

are amphoteric and positively charged under acidic condition. At pH 3, nonetheless, STN exhibits high sorption capacities for Pb, Cd and Cu (1.27, 0.39 and 0.34 mmol/g, respectively). The calculated Langmuir sorption capacities and constants are listed in Table 1. As shown in Fig. 1, the order of STN sorption capacity for divalent cations is Pb ≫ Cd > Cu > Zn > Ca > Sr > Ni. Sequences of sorption capacities are unique to each sorbent. Hydrous manganese oxide has the order of Pb > Cu > Zn > Ni > Cd > Sr > Ca [17] while hydrous ferric oxide has binding sequence of Pb > Cu > Cd > Zn > Ni > Ca [18]. Generally, transition and post-transition cations tend to have better binding affinity than alkaline earth cations. According to the hard and soft acids and bases (HSAB) theory, transition and post-transition cations are either soft or borderline acids whereas alkaline earth cations are hard acids [19]. Soft acids have higher acidity and bind more readily to metal oxides than hard acids. They are unaffected by surface charge of sorbent and can bind at low pH even when sites are protonated. In contrast hard acids, such as Ca and Sr, are able to bond only when pH is higher and surface is deprotonated [20]. Despite aqueous hydroxyl (OH^-) being labeled as a hard base [19], the hydroxyl functional groups on STN are different. This is because the oxygen in OH^- sites has additional coordination to titanium atom(s). These local coordinations (singly, doubly or triply), consequentially, increases the affinity for metal cations. As shown in Fig. 1, STN shows higher affinity for relatively softer acids (Pb, Cd, Cu and Zn). Therefore STN should be considered a soft base.

3.2. Kurbatov plot

This empirical method was first presented by Kurbatov et al. [23] to describe sorption behavior as a function of pH. Essentially it is a transformation of sorption edge into a linear curve by plotting log D versus pH. Distribution ratio, D, is the proportion of cation on STN to cation in solution:

$$D = \frac{C_0 - C_e}{C_e}$$

where C_0 and C_e are the initial and equilibrium concentrations of cation (mol/L). The slope of Kurbatov plot describes the ratio of protons and cations exchanged [24]. Intersection of curve with the abscissa is known as pH_{50} (Table S1), the point where log D is zero and sorption efficiency is 50%. Among the divalent cations, Pb is the highest (Fig. 2) and the selectivity is similar to the order observed in isotherms. From Fig. 2, it is evident the plots are *grouped*

Table 1
Langmuir and intrinsic parameters for selected divalent cations.

Divalent cation	Langmuir parameters		pK_{MeOH}[a]	Electro-negativity, χ[b]	Pearson hardness, η[c]	Charge–size function, Z^2/r[d]
	$\log \Gamma_{max}$	$\log K_L$				
Pb	−2.896	6.051	7.60	1.87	8.46	10.30
Cd	−3.412	5.821	10.10	1.69	10.29	9.40
Cu	−3.474	5.034	7.50	2.00	8.27	11.80
Zn	−3.814	4.557	9.00	1.65	10.88	11.70
Ni	−4.708	4.310	9.90	1.91	8.50	12.40
Ca	−3.997	4.377	12.70	1.00	19.52	9.00
Sr	−4.323	4.817	13.18	0.95	16.30	7.80

[a] $pK_{MeOH} = -\log K_{MeOH}$ and K_{MeOH} is hydrolysis constant $Me^{2+} + H_2O \leftrightarrow MeOH^+ + H^+$. From minteq.v4.dat [21].
[b] From Table 5.6 of [19].
[c] From Table 1 of [22].
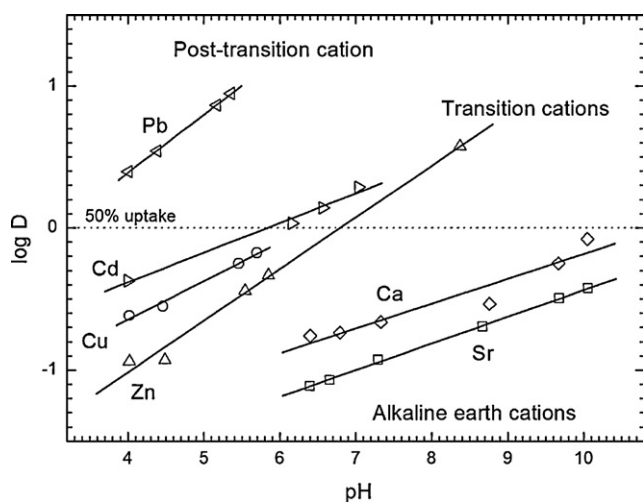[d] $\times 10^{28}$ C^2/m. From Table 9.3 of [19].

together according to their position in the periodic table. Post-transition Pb which has the highest $\log D$ for a given pH, is above the plots of transition cations (Cd, Cu and Zn). The alkaline earth cations (Ca and Sr), which have the least affinity for STN, position towards the bottom right corner of the graph. Generally the slope of each plot (Table S1) is in the decreasing order of post-transition cation > transition cations > alkaline earth cations. The order is in accordance with reported trend [24].

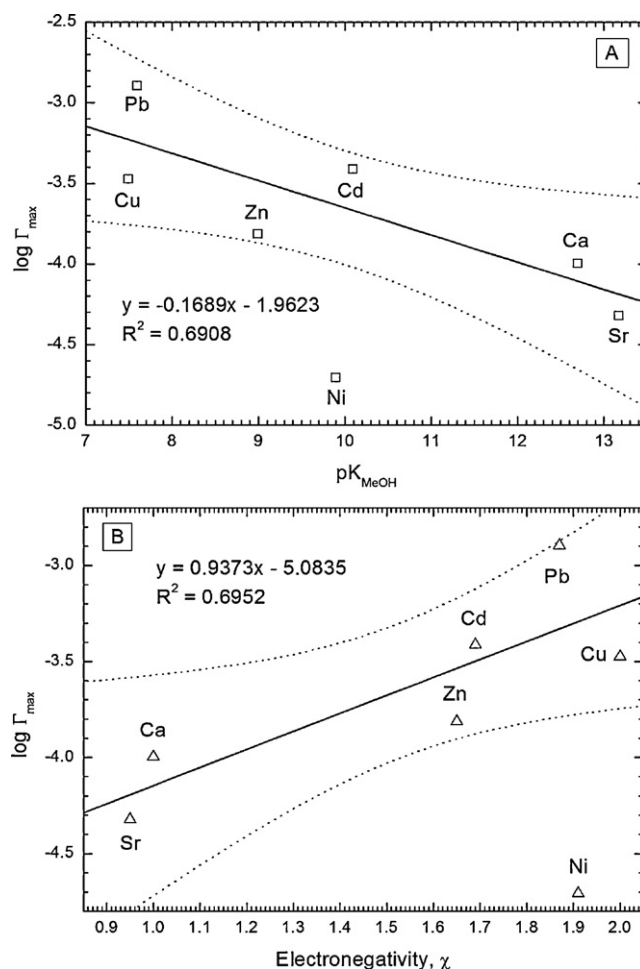### 3.3. Correlation of sorption capacity

To understand the effect of intrinsic cation parameters have on the sorption capacities, the Langmuir parameters (Γ_{max} and K_L) were plotted against the intrinsic parameters listed in Table 1. It was found that $\log \Gamma_{max}$ varies linearly with first hydrolysis constant, pK_{MeOH}, and electronegativity, χ, of the cation. Fig. 3A displays the relationship between $\log \Gamma_{max}$ and pK_{MeOH}. In the semilog plot, the sorption capacity of STN increases with higher hydrolysis constants. As hydrolysis constants describe the affinity of the cation to bond with OH^- and is related to the binding constants of cation onto metal oxide [18] it is reasonable to apply correlation of $\log \Gamma_{max}$–pK_{MeOH} to predict sorption capacities of other divalent cations. Various studies have tried to linearly correlate experimental or modeling results with intrinsic parameters of cations. Dzombak and Morel [18] used linear-free energy relationship to associate hydrous ferrous oxide binding constants with hydrolysis constants. Reddad et al. [25] obtained good fits for linear

regression of sorption rate and sorption capacity with hydrolysis constants of heavy metal cations.

In general electronegativity increases across the periodic table from left to right; alkaline earth cations have lower electronegativities than heavier transition cations. From Fig. 3B, STN have higher capacities for cations with high electronegativities. Electronegativity is defined as the power of an element to attract electrons to itself [19]. Having higher electronegativities, the post-transition and transition cations are preferentially sorbed than alkaline earth cations. The relationship was also observed by other researchers [26,27].

Fig. 3. Correlation of sorption capacity with (A) hydrolysis constant and (B) electronegativity. Linear regression (solid line) and 95% confidence intervals (dotted lines) are shown. Ni was not considered in regression.

Fig. 2. Effect of pH on distribution coefficient, D (Kurbatov plot). STN = 0.005 g/L, I = 0.1 M, cation = 10−5 M. Data points with more than 90% sorption or pH exceeding precipitation were not included in the plot. Linear regression parameters are listed in Table S1.

3.4. Competitive sorption

Due to its toxicity and wide occurrence, it is important to understand the effect of divalent cations have on the sorption of Cd by STN. Percentage of cations being sorbed by STN was calculated by:

$$\text{Sorption efficiency (\%)} = \frac{C_0 - C_e}{C_0} \times 100\%$$

where C_0 and C_e are the initial and equilibrium concentrations of cation (mol/L). Pb has the most pronounced effect on Cd uptake (Fig. 4A). At equimolar concentrations the post-transition cation is preferred over Cd. When Pb is reduced by an order of magnitude, fractional uptake of Cd can be observed. At molar ratio of 1:1 Pb competes with Cd for the limited sites available of STN and with the reduced of Pb ten fold sites become available for sorption of both

Pb and Cd. As mentioned in the earlier section, the high affinity for Pb is also evident in other metal oxides such as manganese oxide and ferric oxide [17,18].

Systems of Cu–Cd and Zn–Cd have similar sorption behaviors (Fig. 4B and C). At equimolar ratio, Cd is preferred over Cu and Zn. Under acidic condition (pH < 5), sorption efficiencies of Cd were the same with and without competing cations. STN preferentially sorbs Cd even when Cu or Zn molarity is increased fivefold. At higher pH, however, the affinity for Cd decreases and increased uptakes of Cu and Zn were observed. Maximum uptake of Cd occurred at pH 6–7 for both systems. As discussed in the Kurbatov plot, STN have similar sorption behavior on all three transition cations with Cd having the highest binding. Hence it is not surprising to find that Cd is preferred over Cu and Zn in the competitive sorption.

Nickel, despite being a transition metal, did not have significant effect on uptake of Cd (Fig. 4D). Sorption edges of Ni–Cd are different
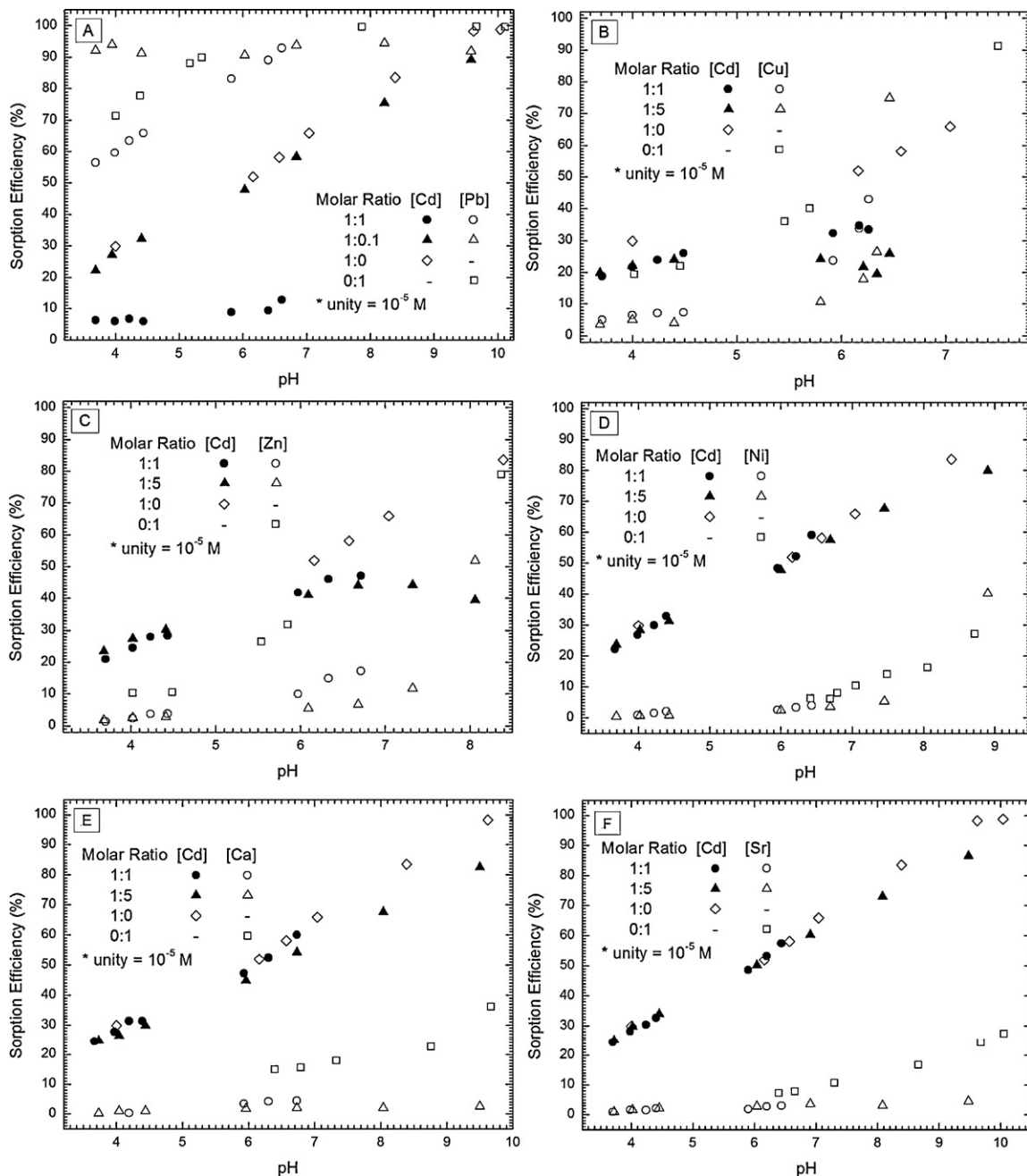

Fig. 4. Competitive sorption between Cd and (A) Pb (B) Cu (C) Zn (D) Ni (E) Ca (F) Sr as a function of pH. STN = 0.005 g/L, I = 0.1 M.

from Cu–Cd and Zn–Cd systems. The presence of Ni did not impede STN uptake of Cd. Five fold increment of Ni did not affect the uptake of Cd significantly either. Uptake of Ni was not observed in competitive sorption systems and while the sudden increase at pH > 8 is attributed to the precipitation of nickel hydroxide. The sorption edges of Ni resemble that of alkaline earth cations (cf. Fig. 4E and F) rather than the transition cations.

In systems of Ca–Cd and Sr–Cd (Fig. 4E and F), STN was more selective towards Cd and its uptake was not affected by Ca or Sr. The effects of alkaline earth cations were insignificant on the uptake of Cd. It was found that increasing either Ca or Sr five fold did not lead to significant change in the sorption efficiency of Cd. The sorption sites on STN were binded by Cd and uptakes of Ca and Sr are negligible. This is explained by the outer-sphere complexes formed on STN by alkaline earth cations [28]. Group II cations binding occur when surface of STN is negatively charged (i.e., pH > PZC). Their bondings with hydroxyl group are outer-sphere complexation due to ionic charges whereas heavy metal cations form inner-sphere complexation, a covalent bonding mechanism [20].

3.5. Anomaly of nickel

In both linear correlations, Ni fell outside the 95% confidence intervals suggesting the usual sorption behavior of Ni on STN. The sorption capacity for Ni is in the same order of magnitude with alkaline earth cations (cf. Table 1) and the HSAB theory is unable to describe its behavior. Being defined as a soft acid, it should bind strongly to OH sites on STN regardless of pH. On the contrary, Kurbatov plot of Ni (Fig. S1) shows sorption was observed only when pH exceeds the PZC of STN. Using extrapolation, other transition cations (Cd, Cu and Zn) have $pH_{50} < pK_{MeOH}$. That is, sorption efficiency of more than 50% is achieved before the first hydrolysis constant. For Ni, substantial uptake occurred only when pH exceeds the pK_{MeOH}. It is plausible that sorption mechanism of Ni on STN is different from the other transition cations. The counter-intuitive behavior of Ni, however, was not observed on other metal oxides [18,24].

4. Conclusion

Sodium titanate nanotubes not only displayed high sorption capacity for toxic heavy metals (Pb and Cd), the novel sorbent but also has unique selectivity for Cd over Zn, Ni, Ca and Sr. The exceptional selectivity indicates STN can be utilized to remove Cd from industrial wastewater, particularly from NiCd batteries manufacturing. In the hypothetical situation where high levels of Pb and Cd are present together, it is recommended that Pb should be precipitated prior to Cd recovery.

Acknowledgements

Appendix A. Supplementary data

Supplementary data associated with this article can be found, in the online version, at doi:10.1016/j.jhazmat.2010.12.120.

References

[1] H.S. Posselt, W.J. Weber, Environmental Chemistry of Cadmium in Aqueous Systems, University of Michigan, Dept. of Civil Engineering, 1971, p. 178.

[2] L.E. Hetherington, T.J. Brown, A.J. Benham, T. Bide, P.A.J. Lusty, V.L. Hards, S.D. Hannis, N.E. Idoine, World Mineral Production 2002–06, British Geological Survey, Keyworth, Nottingham, 2008.

[3] K.F. Lam, K.L. Yeung, G. McKay, Efficient approach for Cd^{2+} and Ni^{2+} removal and recovery using mesoporous adsorbent with tunable selectivity, Environmental Science and Technology 41 (2007) 3329–3334.

[4] A.C. Tolcin, Mineral commodity summaries – cadmium, in: U.S. Geological Survey 2010, 2010, p. 36.

[5] http://www.epa.gov/safewater/contaminants/index.html, 11 June 2010.

[6] M. Kasuya, Recent epidemiological studies on itai-itai disease as a chronic cadmium poisoning in Japan, Water Science and Technology 42 (2000) 147–154.

[7] M.P. Waalkes, Cadmium carcinogenesis, Mutation Research: Fundamental Molecular Mechanisms of Mutagenesis 533 (2003) 107–120.

[8] A. Demirbas, E. Pehlivan, F. Gode, T. Altun, G. Arslan, Adsorption of Cu(II), Zn(II), Ni(II), Pb(II), and Cd(II) from aqueous solution on Amberlite IR-120 synthetic resin, Journal of Colloid and Interface Science 282 (2005) 20–25.

[9] J.B Brower, R.L. Ryan, M. Pazirandeh, Comparison of ion-exchange resins and biosorbents for the removal of heavy metals from plating factory, Wastewater, Environmental Science and Technology 31 (1997) 2910–2914.

[10] T. Kasuga, M. Hiramatsu, A. Hoson, T. Sekino, K. Niihara, Formation of titanium oxide nanotube, Langmuir 14 (1998) 3160–3163.

[11] H.Y. Niu, J.M. Wang, Y.L. Shi, Y.Q. Cai, F.S. Wei, Adsorption behavior of arsenic onto protonated titanate nanotubes prepared via hydrothermal method, Microporous and Mesoporous Materials 122 (2009) 28–35.

[12] S.-S. Liu, C.-K. Lee, H.-C. Chen, C.-C. Wang, L.-C. Juang, Application of titanate nanotubes for Cu(II) ions adsorptive removal from aqueous solution, Chemical Engineering Journal 147 (2009) 188–193.

[13] D.J. Yang, Z.F. Zheng, H.Y. Zhu, H.W. Liu, X.P. Gao, Titanate nanofibers as intelligent absorbents for the removal of radioactive ions from water, Advanced Materials 20 (2008) 2777.

[14] D.V. Bavykin, F.C. Walsh, Kinetics of alkali metal ion exchange into nanotubular and nanofibrous titanates, Journal of Physical Chemistry C 111 (2007) 14644–14651.

[15] D.V. Bavykin, K.E. Redmond, B.P. Nias, A.N. Kulak, F.C. Walsh, The effect of ionic charge on the adsorption of organic dyes onto titanate nanotubes, Australian Journal of Chemistry 63 (2010) 270–275.

[16] H.H. Ou, C.H. Liao, Y.H. Liou, J.H. Hong, S.L. Lo, Photocatalytic oxidation of aqueous ammonia over microwave-induced titanate nanotubes, Environmental Science and Technology 42 (2008) 4507–4512.

[17] J.W. Tonkin, L.S. Balistrieri, J.W. Murray, Modeling sorption of divalent metal cations on hydrous manganese oxide using the diffuse double layer model, Applied Geochemistry 19 (2004) 29–53.

[18] D. Dzombak, F.M.M. Morel, Surface Complexation Modeling, Wiley-Interscience, New York, 1990.

[19] J.E. Huheey, E.A. Keiter, R.L. Keiter, Inorganic Chemistry: Principles of Structure and Reactivity, fourth ed., HarperCollins College, New York, 1993.

[20] K.F. Hayes, Equilibrium, Spectroscopic and Kinetic Studies of Ion Adsorption at the Oxide/Aqueous Interface, Stanford University, 1987.

[21] J.D. Allison, D.S. Brown, K.J. Novo-Gradac, MINTEQA2, A Geochemical Assessment Model for Environmental Systems, U.S. Environmental Protection Agency, Athens, GA, 1991.

[22] R.G. Pearson, Absolute electronegativity and hardness: application to inorganic chemistry, Inorganic Chemistry 27 (1988) 734–740.

[23] M.H. Kurbatov, G.B. Wood, J.D. Kurbatov, Isothermal adsorption of cobalt from dilute solutions, Journal of Physical Chemistry 55 (1950) 1170–1182.

[24] D.G. Kinniburgh, M.L. Jackson, Cation adsorption by hydrous metal oxides and clay, in: M.A. Anderson, A.L. Rubin (Eds.), Adsorption of Inorganics at Solid–Liquid Interfaces, Ann Arbor Science Publishers, Ann Arbor, 1981.

[25] Z. Reddad, C. Gerente, Y. Andres, P. Le Cloirec, Adsorption of several metal ions onto a low-cost biosorbent: kinetic and equilibrium studies, Environmental Science and Technology 36 (2002) 2067–2073.

[26] C. Faur-Brasquet, Z. Reddad, K. Kadirvelu, P. Le Cloirec, Modeling the adsorption of metal ions (Cu^{2+}, Ni^{2+}, Pb^{2+}) onto ACCs using surface complexation models, Applied Surface Science 196 (2002) 356–365.

[27] S.J. Allen, P.A. Brown, Isotherm analyses for single component and multi-component metal sorption onto lignite, Journal of Chemical Technology and Biotechnology 62 (1995) 17–24.

[28] R.P.J.J. Rietra, T. Hiemstra, W.H. Van Riemsdijk, Interaction between calcium and phosphate adsorption on goethite, Environmental Science and Technology 35 (2001) 3369–3374.